JOURNAL OF SOLID STATE CHEMISTRY **123,** 249–254 (1996)
ARTICLE NO. 0175

Autocatalytic Reduction of Hematite with Hydrogen under Conditions of Surface Control: A Vacancy-Based Mechanism

M. H. Abd Elhamid, M. M. Khader, A. E. Mahgoub, B. E. El Anadouli, and B. G. Ateya[1]

Chemistry Department, Faculty of Science, Cairo University, Cairo, Egypt

Received October 16, 1995; in revised form February 2, 1996; accepted February 19, 1996

An autocatalytic mechanism is shown to explain the kinetics of the surface reaction occurring during the low-temperature reduction of sintered hematite pellets with hydrogen between 300 and 500°C. The results satisfactorily fit the predictions of a mechanism based on nondissociative chemisorption of hydrogen on the oxygen vacancies at the surface of the hematite pellet. This chemisorption process activates the hydrogen molecule by substantially decreasing its bond energy and increasing its bond length. The calculated activation energy of the surface reaction over this temperature range was found to be much smaller than those reported earlier. The larger values are believed to have been affected by some diffusion control within the solid phase, as a result of the limitations of the weight loss technique which was used in those measurements. © 1996 Academic Press, Inc.

INTRODUCTION

The reduction of ferric oxide has been studied extensively (1–10) in view of its importance to iron making and steel making. Furthermore, a study of the kinetics of this reaction reveals much useful information on the nature of ferric and lower iron oxides. The issue also bears on the use of ferric oxide in catalysis (11, 12) and on its potential as a thermistor (13), a gas sensor (14), and as a photoanode in solar energy conversion devices (15).

The kinetics of reduction of Fe_2O_3 were frequently studied by measuring its weight loss (7–11, 16–22). The extent of the reduction was often expressed in terms of the fraction or the degree of reduction (x) which is the ratio of the measured weight loss at a certain time to the total theoretical weight loss which is attainable after the entire sample has undergone reduction to the extent required by the prevailing thermodynamics. With this definition, $0 < x < 1$. The experimental results are presented as x–t plots for various parameters, e.g., pellet thickness or diameter, reduction temperature, etc. The major part of the kinetic analyses reported in the literature is based on measurements involving significant x values, i.e., $x > 0.1$. The weight loss technique is not sensitive enough to detect small changes in the oxide ion concentration during the initial stage of the reduction process, i.e., under the conditions of surface control, particularly at low temperatures, e.g., below 500°C.

Alternatively, various workers performed measurements of the electrical conductivity of ferric oxide pellets during reduction (12, 14, 23). The conductivity was shown to increase by up to some orders of magnitude during the reduction process. Furthermore, the extent of these variations was found to depend on the gas composition, reduction temperature, and pellet thickness. This technique is particularly useful during the early stages of the reduction process, where the weight loss is negligibly small. It is shown below that the onset of diffusion control occurs at $x < 0.01$ and that the present technique can measure x values accurately down to $x = 10^{-5}$.

The aim of this paper was to study the kinetics of the surface reaction during the reduction of ferric oxide pellets with hydrogen. This is achieved via measurement of the electrical conductivity of the pellets during the course of reduction. In view of the results of earlier workers (24–26), the increase in conductivity was attributed to an increase in the density of oxygen vacancies which results from the reduction reaction. The results are confined to the low-temperature region (≤500°C) where the reduction product is a lower oxide, i.e., magnetite. This region attracted much less attention in the literature than the high-temperature region where the reduction product is metallic iron. It is also particularly relevant to the processes occurring in the upper part of the blast furnace. An autocatalytic mechanism, promoted by the oxygen vacancies, is proposed to explain and analyze the results.

EXPERIMENTAL

The pellets used in this work were prepared from ferric oxide powder (Alfa products, 99.99%). The powder was compressed in the form of pellets using a stainless steel die and a hydraulic press at 10 ton cm^{-2}. The pellets had

[1] To whom correspondence should be addressed.

0022-4596/96 $18.00

a diameter of 1.3 cm and a thickness of 0.1 cm. They were sintered in air for 24 hr at 800°C, and air-cooled to room temperature.

A simple conductivity cell was made from circular shaped platinum electrodes of the same diameter as the ferric oxide pellet. These were made of platinum screens, to allow easy access of the reducing gas to the surface of the pellet. Electrical leads were spot-welded to the platinum screens. Tight contact between the electrodes and the pellet was maintained by pressing the assembly using two stainless steel disks and a pressure spring. A Chromel-Alumel thermocouple was used to measure the temperature, which was adjusted to ∓ 5°C. The sintered pellets were mounted between the two Pt electrodes of the conductivity cell and held tightly with the spring. The cell holder was placed in a Pyrex tube with inlet and outlet ports for hydrogen. This assembly was positioned inside a horizontal tube furnace. The electrical conductivity was measured with an EG & G Princeton Applied Research Model 363 electrometer using the current–voltage technique. The electrical power on the sample was limited to 0.1 W cm^{-3} to prevent excessive Joule heating.

After the desired temperature was established for about 1 hr, the measurement of conductivity was started. The measured value at this stage is the conductivity of the bulk stoichiometric material, σ_b. A stream of hydrogen gas was allowed to flush the cell at the desired temperature and the conductivity was measured as a function of the reduction time. The hydrogen gas was generated by water electrolysis at 75°. The resulting stream of hydrogen gas had a partial pressure of 0.65 atm.

RESULTS AND DISCUSSION

The variation of the electrical conductivity of the pellets with the time of reduction is shown in Fig. 1 for various reduction temperatures. The conductivity increases with the time of reduction in a rather complex manner reaching limiting values at sufficiently long reduction times. These limiting values are the conductivities of magnetite which is the reduction product that is thermodynamically stable under the prevailing conditions of temperature and hydrogen gas pressure (9, 27–29). Note that the logarithmic scale gives the fine details of the changes in conductivity with time. It will be shown below that the conductivity is a measure of the extent of reduction. Consequently, the degree of reduction x at a certain time is taken as the ratio between the conductivity measured at this time and the limiting value corresponding to the plateau in Fig. 1, i.e., the conductivity of magnetite at the particular temperature. Thus,

$$x = \sigma(t)/\sigma_\infty \qquad [1]$$

This (x) value is marked on the right side of Fig. 1. The results of Fig. 1 show that with the present technique it is possible to measure degrees of reduction as low as 10^{-5}. The above phenomenological definition of x requires that $x = 1$ when Fe_2O_3 is completely reduced to Fe_3O_4, which has a different phase structure. Conversely for very small values of x, e.g., $x < 0.01$, only a thin layer at the pellet surface has been reduced while the interior of the pellet is not affected.

The increase in conductivity is a result of the increase in the number of oxygen vacancies which are generated upon the reduction of Fe_2O_3. This reaction can be represented by

$$O^{2-}(l) + H(g) \rightarrow H_2O(g) + V^{2-}(l), \qquad [2a]$$

where $V^{2-}(l)$ is an oxygen vacancy which results from the removal of an oxide ion $O^{2-}(l)$ from the Fe_2O_3 lattice. The oxygen vacancies form mobile point defects in the crystal structure of Fe_2O_3, leading to an increase in its conductivity. The mechanisms of conduction in hematite and in magnetite are discussed in great detail in the literature (30–34). As more oxygen vacancies are generated, the remaining hematite deviates from stoichiometry. The extent of this deviation can be expressed as δ in the formula $Fe_2O_{3-\delta}$, following Salmon (35). In view of this, reaction [2a] can also be expressed as

$$Fe_2O_3 + \delta H_2(g) \rightarrow Fe_2O_{3-\delta} + \delta H_2O(g), \qquad [2b]$$

where Fe_2O_3 and $Fe_2O_{3-\delta}$ refer to the stoichiometric and the defective oxides, respectively. As more Fe_2O_3 is reduced more oxygen vacancies are produced and hence the electronic conductivity increases. Both quantities are related by the

$$\sigma = 2en\mu, \qquad [3]$$

where e is the charge of the electron, μ is the mobility, and n is the concentration of the oxygen vacancies. As revealed by Eqs. [2a], [2b], and [3], the conductivity increases with time as does the rate of generation of oxygen vacancies.

Figure 1 reveals three distinct regions (for temperatures $\geq$375°C) with different modes of variation of conductivity with the time of reduction, i.e., regions I, II, and III. These occur, respectively, at short, intermediate, and moderately long reduction times. After region III, we reach a limiting conductivity value (plateau) that corresponds to the conductivity of the thermodynamically stable composition of the reduction product, i.e., Fe_3O_4 (9, 27–29) which has a much higher conductivity than Fe_2O_3 (26, 34). Region I starts at $t = 0$ and extends up to the beginning of the inflection of the $\sigma - t$ relations, see Fig. 1. The experimental

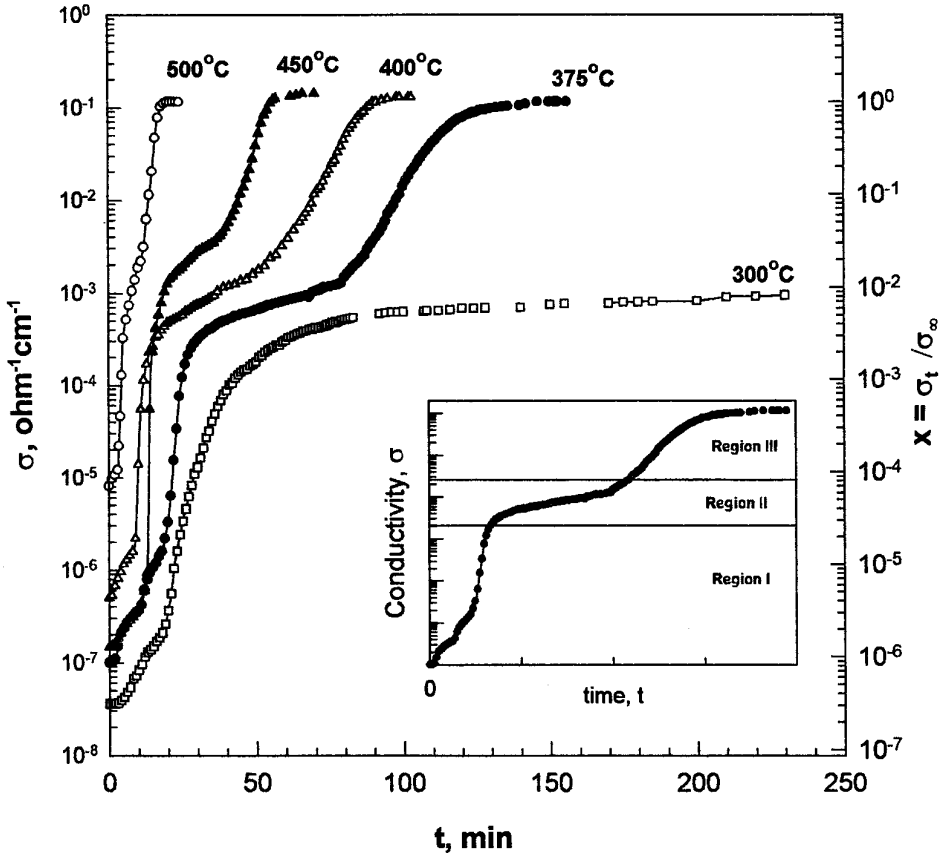

FIG. 1. Plot of ln σ vs reduction time for the pellets of Fe_2O_3 reduced at different reduction temperatures. Insert illustrates regions I, II, and III.

results in this region will be analyzed for the mechanism of the surface reaction, where $x < 10^{-2}$. On the other hand, regions II and III correspond, respectively, to the short and long time diffusion behavior of the system. These will be analyzed and discussed in a later report.

Region I

During region I the conductivity increases rapidly with time, at a rate dependent on the temperature. However the measured conductivity remains about 2–3 orders of magnitude lower than the limiting value. Hence the degree of reduction x varies between the limits $10^{-5} < x < 10^{-2}$. During this initial stage of the reduction process, the reaction is confined to the surface of the pellet. In an earlier work, region I was found to be identical for pellets of 0.05, 0.10, and 0.12 cm thickness (23). This confirms that region I corresponds to the reaction of the pellet surface and excludes the presence of significant pore diffusion. Consequently, the measured conductivity in this region is attributed to the oxygen vacancies in the reduced "skin layer" around the surface of the pellet. At early reaction times, this skin layer is on the order of monolayer in thickness. It furnishes a low resistance short circuit path around the interior of the pellet which retains the stoichiometric composition and, hence, the low conductivity of Fe_2O_3. This surface conductivity is denoted σ_t while the conductivity of the bulk stoichiometric material is denoted σ_b.

Region I starts with an initial induction period, where the conductivity increases with time only slowly, followed by a rather sharp increase of conductivity with the time of reduction. The length of the induction period increases as the reduction temperature decreases. It is also associated with a several-fold increase in the conductivity. At the end of the induction period, the reaction accelerates very rapidly in a manner characteristic of autocatalytic reactions (36–38).

Mechanism of the Surface Reaction

It is recognized that the Fe_2O_3 pellets, before undergoing any reduction, are essentially stoichiometric (25), i.e., they have very low defect density. It is proposed here that hydrogen gas is activated through chemisorption on the oxygen vacancies prior to the reduction of Fe_2O_3, i.e.,

$$H_2(g) + V^{2-}(l) \xrightarrow{\text{fast}} H_2(ads). \qquad [4]$$

The above proposal is compatible with the fact that the diameter of the oxygen ion, which is taken equal to that of the vacancy, is 2.64 Å which is much greater than the diameter of the hydrogen molecule (0.74 Å) (39). The assumption of nondissociative chemisorption of H_2 on hematite is supported by the results of extensive theoretical calculations (40). These calculations revealed that the chemisorption process leads to the softening of the H–H bond, i.e., to an increase in the bond length above its equilibrium value and a decrease in the bond energy by up to about 45 kcal/mol from an original values of about 103 kcal/mol.

The slow step involves a reaction between this activated adsorbed hydrogen and an oxide ion from the Fe_2O_3 lattice giving rise to a freshly generated vacancy and an adsorbed H_2O molecule, i.e.,

$$H_2(ads) + O^{2-}(l) \xrightarrow{slow} V^{2-}(l) + H_2O(ads). \quad [5]$$

Note that reaction [5] involves total rupture of the H–H bond in the H_2 molecule and extraction of an O^{2-} ion from the lattice, hence it is considered the slowest step. The adsorbed H_2O is desorbed off the surface leaving behind another oxygen vacancy, i.e.,

$$H_2O(ads) \xrightarrow{fast} H_2O(g) + V^{2-}(l). \quad [6]$$

The overall reaction is given by

$$H_2(g) + O^{2-}(l) \rightarrow H_2O(g) + V^{2-}(l) \quad [7]$$

This is equivalent to reactions [2a] and [2b]. While reactions [4] and [6] are assumed to be fast, reaction [5] is taken to be the rate determining step. As the reaction proceeds, more oxygen vacancies are generated. Consequently, more hydrogen is adsorbed giving rise to higher reaction rates, which lead to the generation of more vacancies at even higher rates, etc. This mechanism requires that the more defective the hematite, the more reactive it is toward reduction with hydrogen. Such a correlation was amply confirmed before (11).

Within the framework of this mechanism, the reaction rate equals the rate of generation of oxygen vacancies. Thus

$$\frac{dn}{dt} \alpha \theta_{H_2}[O^{2-}]_t, \quad [8]$$

where n is the number of oxygen vacancies, θ_{H_2} is the number of oxygen vacancies covered with adsorbed hydrogen, and $[O^{2-}]_t$ refers to the concentration of the oxide ion in the surface layer of hematite at time t. Since the adsorption of hydrogen gas on the oxygen vacancies is assumed to be fast, it follows that θ_{H_2} is directly proportional to n. Consequently,

$$\frac{dn}{dt} = kn[O^{2-}]_t \quad [9a]$$

$$= kn([O^{2-}]_b - n), \quad [9b]$$

where k is the specific rate constant of the reduction reaction. Note that $[O^{2-}]_t$ decreases with the time of reduction whereas n and σ increase.

Under conditions of surface control, $n \ll [O^{2-}]_b$ as $\sigma_t/\sigma_\infty < 0.1$ (see Appendix 1). Under this condition, Eq. [9b] can be easily integrated to yield

$$\ln \sigma_t = \ln \sigma_b + \bar{k}t, \quad [10]$$

where σ_b is the conductivity of the pellet having the bulk stoichiometric composition and $\bar{k} = k[O^{2-}]_b$ is the apparent rate constant which includes the bulk concentration of oxide ions. Thus, a plot of $\ln \sigma_t$ vs t within region I should give a straight line, the slope of which equals $\bar{k}$. Alternatively, Eq. [10] can be expressed as

$$n(t) = n_b \exp(\bar{k}t), \quad [11]$$

i.e., the number of oxygen vacancies at the surface of the pellet increases exponentially with time.

When the number of vacancies at the pellet surface reaches the value required by the prevailing thermodynamics, the reduction process will be supported by diffusion of oxide ions from within the bulk to the surface of the pellet and/or by diffusion of vacancies in the opposite direction. This marks the onset of diffusion control on the rate of the reduction process. The analysis of this diffusion problem will be reported later.

Figures 2a–2e illustrate plots of the data of region I according to Eq. [10], for various reduction temperatures. The plots give satisfactory straight lines with a slope equal to the apparent standard rate constant, which increases with the reduction temperature. Figure 3 is an Arrhenius plot of this rate constant. The results fit a satisfactory straight line, with an activation energy of only 7.2 kcal/mol. This is a rather low value as compared to the values reported in the literature for the same process, e.g., 27.3 (8), 17.7 (11), and 13.5 kcal/mol (23, 29). The difference may be attributed to two reasons:

(a) The fact that the calculations of the present work are based on measurements at very small degrees of reduction, i.e., $10^{-5} < x < 10^{-2}$ while earlier works involved substantial x values i.e., $x > 0.1$. Under such conditions, one expects contributions from diffusion limitations within the solid to the measured activation energy.

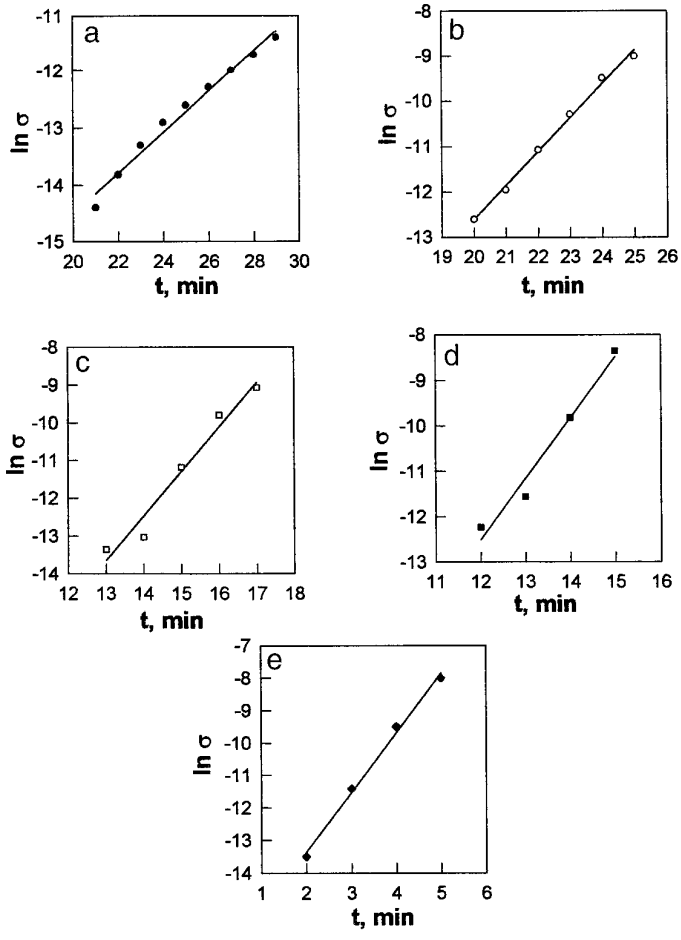

FIG. 2. Plot of ln σ vs time (within region I) for pellets of Fe_2O_3 reduced at (a) 300°C, (b) 375°C, (c) 400°C, (d) 450°C, and (e) 500°C, respectively. The data are taken from region I of Fig. 1.

(b) While some of the previous measurements were taken over sufficiently long times to insure the formation of the bulk magnetite phase, the present results were confined to reduction over relatively short times where only a fairly thin skin layer around the surface of the pellet has been reduced. It is hard to assess the extent of the possible effect of phase transformation on the activation energy measured in this work.

CONCLUSIONS

The results of the present work indicate that the reactivity of hematite toward reduction with hydrogen is determined by the extent of its deviation from stoichiometry, i.e., by the value of δ in the formula $Fe_2O_{3-\delta}$. The value of δ is also a measure of the density of the oxygen vacancies in the hematite lattice. The key assumptions in the proposed autocatalytic mechanism are fast nondissociative chemisorption of H_2 on the oxygen vacancies in the hematite lattice and slow reaction of this chemisorbed hydrogen with the oxide ion. Both assumptions are compatible with experimental and theoretical findings, i.e., (i) the higher reduction temperature reported for hematites prepared in oxygen or inert atmospheres compared to the values reported for hematites prepared in reducing atmospheres (11), (ii) extensive calculations on the chemisorption of H_2 on hematite clusters (40), (iii) the application of autocatalytic mechanisms to the reduction of other oxides (36–38), and (iv) the good agreement between the predictions of the mechanism and the experimental results measured in the present work.

The present work calls for further measurements to test the various aspects of the proposed mechanism, e.g., measurements on hematite with different δ values, and evaluation of the effects of water vapor, partial pressure of hydrogen and other gases which adsorb on hematite competitively with hydrogen.

APPENDIX 1

At the beginning of the reduction process the concentration of the oxide ion equals the bulk (stoichiometric) value $[O^{2-}]_b$ which is large, while the density of oxygen vacancies n, and hence the conductivity σ, are low. As the reduction proceeds, $[O^{2-}]_t$ decreases while n and σ increase. At the limiting value of conductivity (σ_∞, see Fig. 1), $[O^{2-}]_t$ reaches its minimum value as required by the thermodynamics of the process, i.e., $[O^{2-}]_\infty$ while n_∞ and σ_∞ reach their maximum values. In view of the above arguments, it follows that

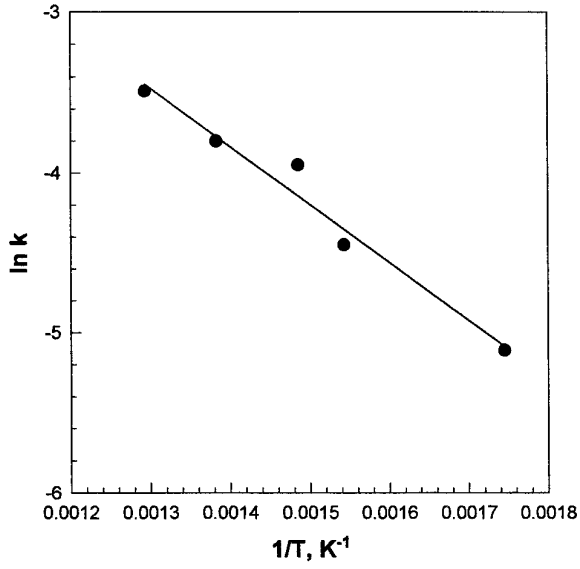

FIG. 3. Arrhenius plot of the standard rate constant $k(T)$ for the surface reaction of Fe_2O_3 pellets reduced at different reduction temperatures.

$$[O^{2-}]_b = [O^{2-}]_t + n, \quad [A.1]$$

i.e.,

$$n = [O^{2-}]_b - [O^{2-}]_t. \quad [A.2]$$

The combination of Eqs. [A.2] and [3] yields

$$\sigma_t = \mu e\{[O^{2-}]_b - [O^{2-}]_t\} \quad [A.3]$$

and

$$\alpha_\infty = \mu e\{[O^{2-}]_b - [O^{2-}]_\infty\}. \quad [A.4]$$

Dividing Eq. [A.3] by Eq. [A.4], one obtains

$$\frac{\sigma_t}{\sigma_\infty} = \frac{[O^{2-}]_b - [O^{2-}]_t}{[O^{2-}]_b - [O^{2-}]_\infty}. \quad [A.5]$$

Taking $[O^{2-}]_\infty \ll [O^{2-}]_b$, Eq. [A.5] yields

$$\frac{\sigma_t}{\sigma_\infty} = 1 - \frac{[O^{2-}]_t}{[O^{2-}]_b}. \quad [A.6]$$

Equation [A.6] indicates that for region I where $[O^{2-}]_b \gg n$ the ratios of $\sigma_t/\sigma_\infty \ll 0.1$, and the ratio $[O^{2-}]_t/[O^{2-}]_b \simeq 1$, i.e., there are no significant changes in the concentration of oxide ion. This clearly corresponds to region I in Fig. 1. During region I, $\sigma_t/\sigma_\infty < 0.01$, i.e., $[O^{2-}]_t = [O^{2-}]_b$ and hence $n \ll [O^{2-}]_b$.

REFERENCES

1. L. Von Bogdandy and H. J. Engell, "The Reduction of Iron Ores." Springer Verlag, Berlin/New York, 1971.
2. H. U. Ross, *in* "Direct Reduced Iron, Technology, and Economics of Production and Use" (R. L. Stephenson and R. M. Smailer, Eds.), p. 26. Iron and Steel Society of the AIME, Warrendale, Pennsylvania, 1980.
3. Y. Omari, "Blast Furnace Phenomena and Modeling." Elsevier Applied Science, London, 1987.
4. J. Szekely, J. W. Evans, and H. Y. Sohn, "Gas-Solid Reactions." Academic Press, New York, 1976.
5. E. T. Turkdogan, "Physical Chemistry of High Temperature Technology." Academic Press, New York, 1980.
6. C. Gleitzer, *Solid State Ionics* **38,** 133 (1990).
7. C. E. Loo and N. J. Bristo, *Trans. Inst. Min. Metall. Sect. C* **103,** C126 (1994).
8. O. J. Wimmers, P. Arnoldy, and J. A. Monjilin, *J. Phys. Chem.* **90,** 1331 (1986).
9. U. Coulombo, F. Gazzarini, and G. Lanzaveccia, *Mater. Sci. Eng.* **2,** 117 (1967).
10. T. Usui, M. Ohmi, S. Kaneda, M. Ohmasa, and Z-I. Morita, *ISIJ Int.* **31,** 425 (1991).
11. M. Shimokawabe, R. Furuichi, and T. Ishii, *Thermochim. Acta* **28,** 287 (1979); *Thermochim. Acta* **24,** 69 (1978); *Thermochim. Acta* **21,** 237 (1977).
12. K. H. Kim and J. S. Choi, *J. Phys. Chem.* **85,** 2447 (1981).
13. J. Certo, C. S. Furtado, A. R. Ferreira, and J. M. Perigao, *J. Eur. Cer. Soc.* **11,** 401 (1993).
14. A. A. Vasiliev and M. A. Polykarpov, *Sensors and Actuators B* **7,** 626 (1992).
15. M. Anderman and J. H. Kennedy, *in* "Semiconductor Electrodes" (H. O. Finkelea, Ed.). Elsevier, Amsterdam, 1988.
16. K. M. Hutchings, J. D. Smith, S. Yoruk, and R. J. Hawkins, *Ironmaking Steelmaking* **14,** 103 (1987).
17. J. M. Quets, M. E. Wadsworth, and J. R. Lewis, *Trans. AIME* **221,** 1186 (1961).
18. N. Towhidi and J. Szekely, *Ironmaking Steelmaking* **6,** 237 (1981).
19. W. M. McKewan, *Trans. AIME* **2,** 218 (1960).
20. A. Baraka, M. E. Ibrahim, Y. Barkat, and M. Selim, *Ann. Chim.* **73,** 433 (1983); *Ann. Chim.* **72,** 623 (1982).
21. U. F. Chinje and J. H. E. Jeffes, *Ironmaking Steelmaking* **17,** 317 (1990).
22. A. A. El-Geassy, K. A. Shehata, and S. Y. Ezz, *Iron Steel Int.* **50,** 329 (1977).
23. M. M. Khader, B. E. EL Anadouli, E. EL-Naggar, and B. G. Ateya, *J. Solid State Chem.* **93,** 283 (1991).
24. D. J. M. Bevan, J. P. Shelton, and J. S. Anderson, *J. Chem. Soc.* 1729 (1984).
25. R. F. G. Gardner, F. Sweetand, and D. W. Tanner, *J. Phys. Chem. Solids* **24,** 1183 (1963).
26. P. Kofstad, "Nonstoichiometry, Diffusion and Electrical Conductivity in Binary Metal Oxides, p. 235. Wiley–Interscience, New York, 1972.
27. J. O. Edstrom, *J. Iron Steel Inst., London* **75,** 289 (1953).
28. M. J. Graham, D. A. Channing, G. A. Swallow, and R. D. Jones, *J. Mater. Sci.* **10,** 1175 (1975).
29. W. M. McKewan, *Trans. AIME* **140,** 221 (1961).
30. R. H. Chang and J. B. Wagner, *J. Am. Ceram. Soc.* **55,** 211 (1972).
31. K. Hoshino and N. L. Peterson, *J. Phys. Chem. Solids* **46,** 375 1247 (1985).
32. A. Atkinson and R. I. Taylor, *J. Phys. Chem. Solids* **46,** 469 (1985).
33. C. R. A. Catlow, J. Corish, J. Hennessy, and W. C. Mackrodt, *J. Am. Ceram. Soc.* **71,** 42 (1988).
34. N. Tsuda, K. Nasu, A. Yansa, and K. Siratori, *in* "Electronic Conduction in Oxides," Springer Series in Solid State Science, Vol. 94, p. 207. Springer-Verlag, Berlin, 1991.
35. O. N. Salmon, *J. Phys. Chem.* **65,** 550 (1961).
36. Frank Wilkinson, "Chemical Kinetics and Reaction Mechanisms." Van Nostrand, New York, 1980.
37. J. Sloczynski and W. Bobinski, *J. Solid State Chem.* **92,** 420 (1992).
38. M. M. Khader, F. M. El-Kheiri, B. E. El Anadouli, and B. G. Ateya, *J. Phys. Chem.* **97,** 6074 (1993).
39. R. C. Weast (Ed.), "Handbook of Chemistry and Physics." CRC Press, Boca Raton, Florida, 1988.
40. L. J. Rodriguez, F. Ruette, and M. Rosa-Brussin, *J. Mol. Catal.* **62,** 199 (1990).